

MAGNETO-CAPACITANCE-VOLTAGE MEASUREMENTS OF ELECTRONS IN WIDE PARABOLIC QUANTUM WELLS

M. Sundaram, K. Ensslin, A. Wixforth*, and A. C. Gossard

Department of Electrical and Computer Engineering, and Materials Department
University of California, Santa Barbara, CA 93106, USA

We report here on the properties of quasi 3-dimensional electron gases (3DEGs) probed via magneto-capacitance-voltage (MCV) measurements. The 3DEGs are realized in wide parabolic quantum wells grown by molecular beam epitaxy of precisely graded $\text{Al}_x\text{Ga}_{1-x}\text{As}$, into which electrons are introduced by modulation doping. This technique results in a good approximation of a high-quality uniform 3-dimensional electron gas or jellium. Predictions of electrical and optical properties for jellium can therefore be tested. The system furthermore has implications for the case of quantum wires and boxes where the electron-confining potential, in most cases, is approximately parabolic. A number of these 3DEGs with 3D densities ranging from $\approx 4 \times 10^{15} \text{ cm}^{-3}$ to $\approx 8 \times 10^{16} \text{ cm}^{-3}$ have been grown and studied. The measurements have been done at $T=4.2\text{K}$, and in perpendicular and parallel magnetic fields up to 8T. With a front gate electrode on the top surface of the sample we are able to deplete the electrons in the parabolic well by squeezing the width of the 3DEG while retaining a constant 3D density. We also simultaneously depopulate the electrical subbands in this multi-subband system. In contrast to a 2DEG at a single interface we observe a monotonic decrease in the measured capacitance with increasing negative bias at all magnetic fields, and for all samples. A self-consistent solution of the Poisson-Schrödinger equation for our system explains this decreasing capacitance very well, but not the weak oscillations that appear at the points of subband depopulation. The MCV trace for electrons in a very narrow ($\approx 750\text{\AA}$ -wide) parabolic quantum well shows pronounced minima corresponding to different subband filling factors at different magnetic fields with one high filling factor appearing earlier than filling factors 2 and 4. Multiple-subband occupancy causes the Shubnikov-de-Haas oscillations in the longitudinal resistance to exhibit non-periodic structure due to a beating in the density of states at the Fermi energy. The measured mobility vs sheet density behaves differently than for a 2DEG.

1. INTRODUCTION

The concept of producing a thick (several hundred Angstroms) 3-dimensional electron gas (3DEG) with

quasi-uniform electron density distribution and high mobility by introducing electrons via remote doping into a parabolic potential well obtained by tailoring the Al composition x_{Al} in an MBE (Molecular Beam Epitaxy)-grown $\text{Al}_x\text{Ga}_{1-x}\text{As}$ alloy¹, has been exploited in the last two years^{2,3}. Such a high-mobility 3DEG is of great interest because it is the closest approximation to the theoretical construct of jellium, a uniform electron

* Now at Sektion Physik, LMU, 8000 München 22, Federal Republic of Germany.

gas residing in a background of constant positive charge. At high magnetic fields and low temperatures helium is predicted to undergo a transition to a spin-density wave state with highly anisotropic electrical properties⁴, and at higher fields still it is predicted to condense into a Wigner crystal⁵. Experimental confirmation of these theories has been fruitless mainly because of the magnetic freezeout and/or high ionized-impurity scattering suffered by electrons in the structures studied which for the most part were doped semiconductors where the electrons resided in the vicinity of positively-charged donor ions.

Using modulation-doping to spatially separate the electrons from the donor ions, and a parabolic potential well to mimic a constant positive charge background², high-mobility 3DEGs with 3D densities below the GaAs metal-insulator-transition density have been grown and their electrical^{6,7} and optical⁸ properties studied with results that have stimulated much theoretical study of this system^{9,10}. The curvature of the parabolic potential determines the 3D density of the 3DEG, allowing a range of densities from $4 \times 10^{15} \text{ cm}^{-3}$ to $8 \times 10^{16} \text{ cm}^{-3}$ to be experimentally realized.

We report here on the electrical properties of this 3DEG in a wide parabolic quantum well probed via Capacitance-Voltage measurements¹¹ at different magnetic fields (MCV).

Inasmuch as the electrons usually occupy 3-4 electrical subbands in the well, such a gas is not an ideal 3DEG. But theory and experiments show that once more than one subband is occupied the Fermi energy of the system is essentially pinned with respect to the bottom of the lowest subband, a characteristic of a 3D system.

2. EXPERIMENTAL DETAILS

Two samples are studied here: PB24, which has a 4640 \AA -wide parabolic well with Al mole fraction x_{Al} going from 0 at the center to 0.3 at the edges with a curvature that would produce a 3DEG with 3D density of $6.0 \times 10^{15} \text{ cm}^{-3}$ in the well, and PB25, which is a narrower 750 \AA -wide parabolic well with the mole fraction going from 0 at the center to 0.1 at the edges with a curvature of $7.8 \times 10^{16} \text{ cm}^{-3}$. In this second sample the x_{Al} further jumps to 0.3 in the barriers providing a square-well-like confinement when the well is filled with electrons.

Both samples were grown in a Varian Gen II MBE machine on semi-insulating LEC GaAs

substrates at substrate temperatures of $\approx 580^\circ\text{C}$ with enough doping provided to fill the well and to allow for surface depletion effects. The parabolic wells were themselves realized using the pulsed Al beam technique¹².

Electron mobility (μ) and sheet density (N_s) vs temperature (T) for both 3DEGs were measured using low magnetic field ($\pm 0.5\text{T}$) Hall measurements in a Van der Pauw geometry on circular mesas prior to evaporation of gates on the sample surfaces. Gold gate electrodes were then evaporated to cover these mesas and low temperature ($T=4.2\text{K}$) capacitance (C) vs gate voltage (V) measurements made between the gate and the 3DEG in the parabolic well, using conventional lockin techniques. The CV measurement schematic is shown in Fig. 1. Measurements were made at constant magnetic fields in steps up to 8T applied both perpendicular to the plane of the 3DEG and in some cases parallel to it.

3. RESULTS & DISCUSSION

Fig. 2 shows μ and N_s vs T for both PB24 (Fig. 2a) and PB25 (Fig. 2b). Insets in the figures show the corresponding parabolic well design parameters. The mobility for both 3DEGs increases with decreasing temperature, attesting to the reduced scattering resulting from the spatial separation between the electrons in the well and the donor ions in the barriers. The low T mobilities are in excess of $10^5 \text{ cm}^2/\text{Vs}$ and

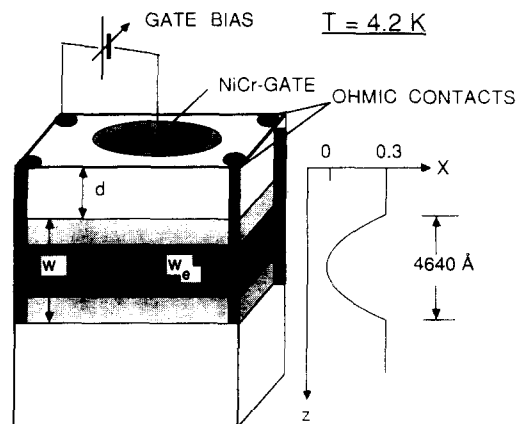


Fig. 1. Schematic of capacitance-voltage measurement showing front gate electrode used to deplete electrons in the 3-dimensional electron gas (3DEG) in the parabolic potential well.

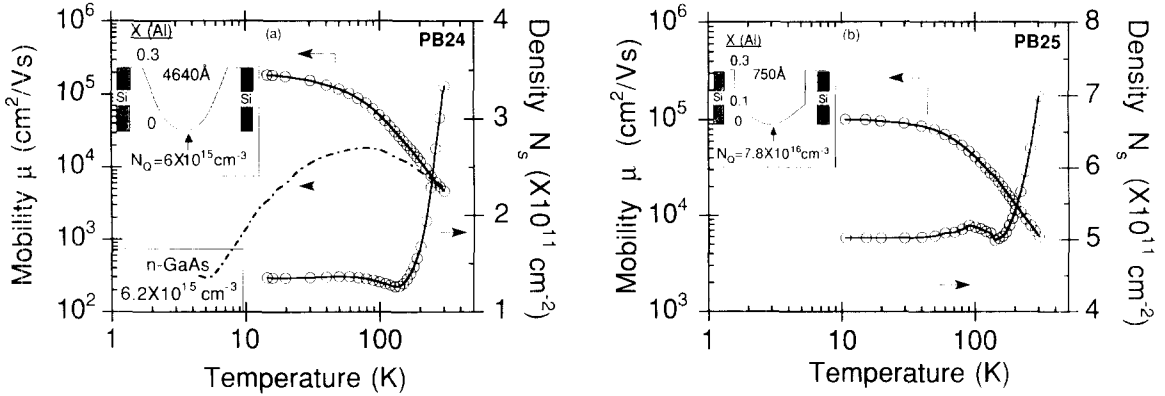


Fig. 2. (a) Temperature dependence of electron mobility and sheet density for 3DEG in 4640Å-wide parabolic well (PB24, shown in inset). Mobility of bulk-doped GaAs with similar 3D density is also shown¹⁴. Note the reduced effect of ionized-impurity scattering at low temperature for electrons in the parabolic well. (b) Temperature dependence of electron mobility and sheet density for 3DEG in 750Å-wide parabolic well (PB25, shown in inset).

the sheet carrier densities N_s saturate at $\approx 1.3 \times 10^{11} \text{ cm}^{-2}$ (classical 3DEG thickness = $N_s/N_Q = 2200 \text{ \AA}$ or 46.7% of the well filled at the uniform 3D density $N_Q = 6 \times 10^{15} \text{ cm}^{-3}$) for PB24, and at $\approx 5.0 \times 10^{11} \text{ cm}^{-2}$ (640Å or 85% of the well filled at $7.8 \times 10^{15} \text{ cm}^{-3}$) for PB25. The scattering mechanism ultimately limiting the low T mobility in these 3DEGs is thought to be the non-specular reflection off the rough walls of the gas of high-mobility electrons whose mean free path is larger than the thickness of the gas¹³. The μ vs T of a similarly bulk-doped GaAs sample¹⁴ is shown in Fig. 2a for comparison and is seen to decrease drastically at low T due to ionized-impurity scattering. Fig. 2a further illustrates the feasibility of realizing 3DEGs with 3D densities below the metal-insulator transition for GaAs ($n_c = 1.6 \times 10^{16} \text{ cm}^{-3}$)¹⁵.

Fig. 3 shows the Al mole fraction profile vs depth for PB24 measured using the ion-gauge of the beam flux monitor in a calibration run immediately prior to actual sample growth in the MBE machine¹⁶. The Al pulses get extremely sharp at the center of the well where x_{Al} approaches zero and the mechanical jitter in the pneumatic shutter used to pulse the Al beam may cause a flat spot with zero curvature to appear at the well-center as evidenced in the same figure.

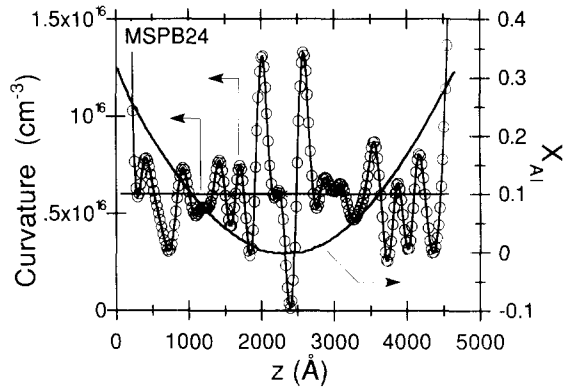


Fig. 3. Measured Al flux profile vs depth for PB24 and the calculated curvature. Note appearance of flat spot (zero curvature) at well-center due to very rapid Al pulses when x_{Al} approaches 0. Horizontal line indicates constant design curvature.

Figs. 4a and 4b show MCV traces for PB24 at constant perpendicular and parallel magnetic fields respectively from 0 Tesla to 8 Tesla in steps of 1 Tesla. C is seen to decrease with negative V, which occurs because of the twin effects of the shrinking width of the

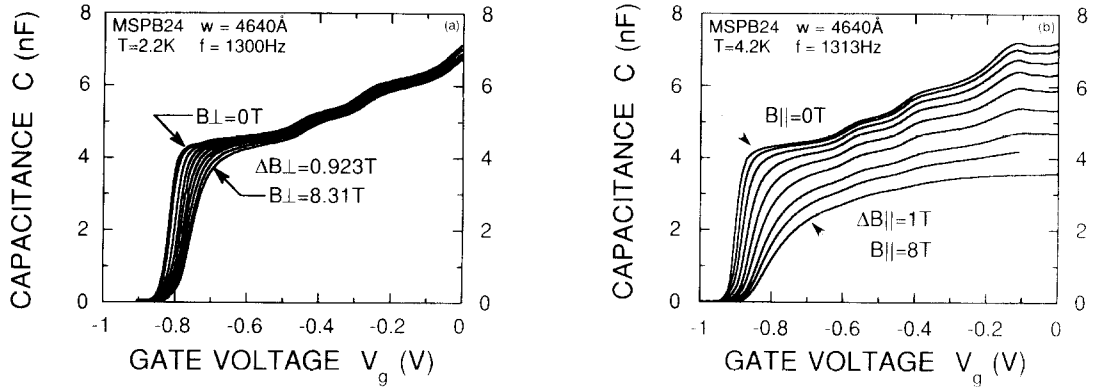


Fig. 4. (a) MCV traces for PB24 at magnetic fields from 0T to 8T in steps of 1T applied perpendicular to sample plane. C decreases with negative bias. Bumps superimposed on this decrease at 0T persist up to 8T. (b) MCV traces at magnetic fields from 0T to 8T in steps of 1T applied parallel to sample plane. Bumps persist up to 6T and do not change much in position along the voltage axis. Only the lowest subband is expected to be occupied above 2T.

3DEG and the driving of its leading edge away from the surface with increasing negative gate bias. Superimposed on this decrease in C from zero gate bias to threshold bias (where all the electrons in the well are depleted) are bumps which persist up to very high perpendicular and parallel magnetic fields and which change little in position along the voltage axis. The position of these bumps is in remarkably good agreement with the positions of subband depopulation at zero field as shown in Fig. 5 which is a calculation of the CV($B=0$) trace from a self-consistent solution of the Poisson-Schrödinger equation for this system. The calculation is done for 4 different temperatures and reproduces the absolute capacitance and the measured decrease very well, but predicts the size of the bumps (due to subband depopulation effects) even at 0K to be a factor of five smaller than observed in the experiment and to be unobservable at 4.2K (the temperature of the measurement). The absolute value of the zero field capacitance measured at any V agrees very well with the plane parallel plate capacitance between the top surface gate and the leading edge of the 3DEG. The subband energies are so closely spaced (less than 1meV)¹¹ at zero field that at the temperature of measurement (4.2K) the 4 lowest subbands are expected to be occupied in perpendicular magnetic fields

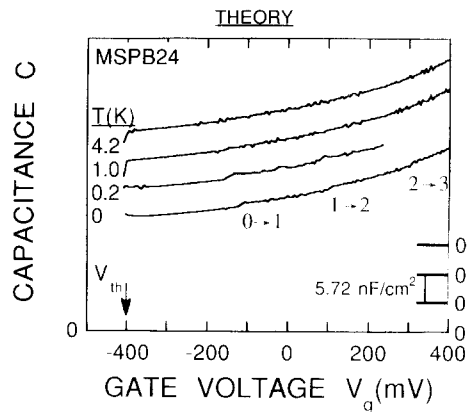


Fig. 5. CV ($B=0$) calculated self-consistently for PB24 for 4 different temperatures. The points of subband depopulation from 4 subbands through 0, along the voltage axis, are shown, and coincide with the positions of the bumps in the experiment. The size of the bumps predicted by this model is very small.

up to 8T. But a parallel magnetic field greater than 2T should magnetically depopulate the higher subbands, leaving all electrons in the lowest one. The fact that the bumps persist in magnitude and are relatively unchanged in position suggests that they might be due

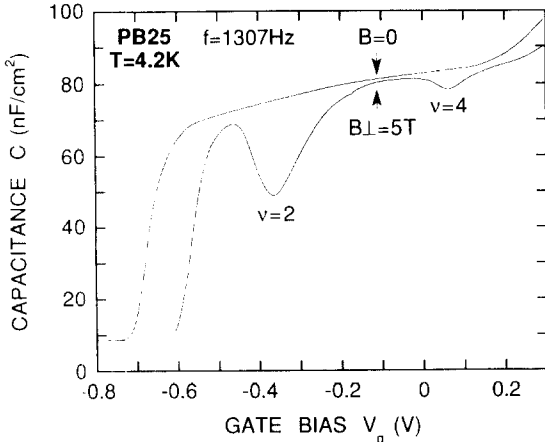


Fig. 6. MCV traces for 0T and for perpendicular field of 5T for electrons in 750Å-wide parabolic well. Minima in the C, due to filling factors 2 and 4 appear in the 5T trace.

at these fields to non-uniformities (enhanced perhaps by e^-e^- interaction) in the electron density distribution produced by flat spots in the well arising from effects described above, or unintentional band-bending by ionized impurities in the well. A self-consistent calculation of the MCV measurement at these fields is obviously needed.

The CV measurement for the narrower PB25 is shown in Fig. 6. Note the decrease in C with increasing negative bias. The absolute values of the measured capacitance at zero field are in agreement with the plane parallel plate capacitance values between gate and leading edge of the 3DEG. Unlike in the wider PB24, no gross features are observed in the 0T trace. On application of a perpendicular magnetic field of 5T two distinct minima are observed. This is due to the changing density of states of the 3DEG as the Fermi energy is swept by the gate bias through the Landau levels (this has been experimentally observed

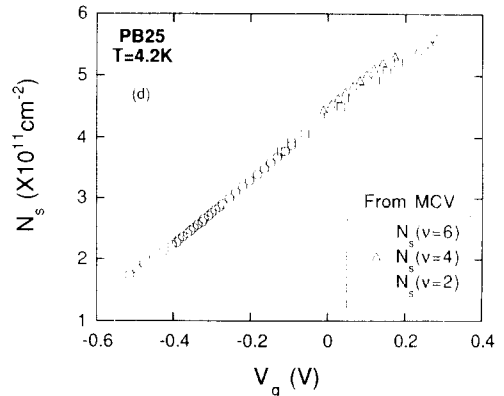
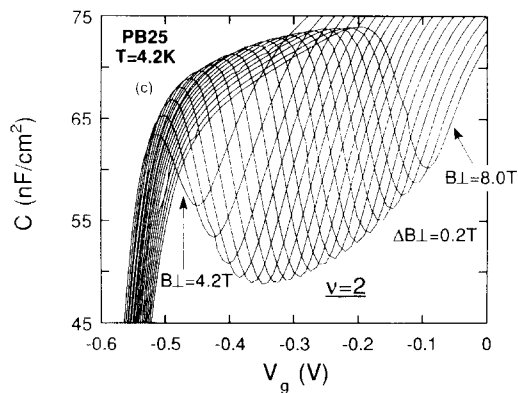
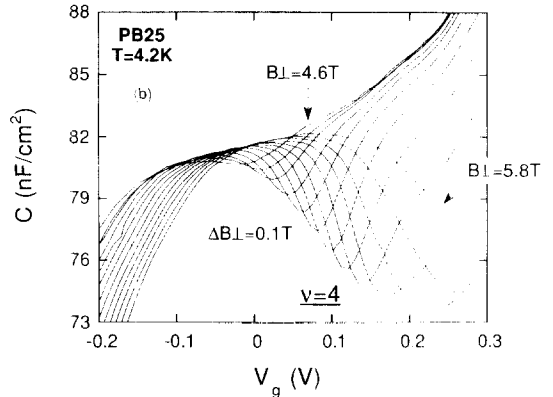
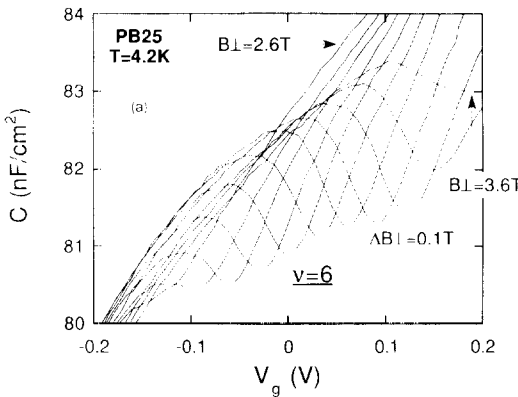


Fig. 7. Tracking the (a) $v=6$, (b) $v=4$, and (c) $v=2$ minima at different perpendicular magnetic fields for PB25. The assignment of $v=6$ to the minimum in (a) is

tentative (see text). It appears at smaller fields than the $v=2$ and $v=4$ minima. (d) N_s vs gate bias calculated from different MCV minima.

in 2DEGs^{17,18}), and corresponds to filling factors 2 and 4.

The evolution of the minima corresponding to filling factors $\nu=6, 4,$ and 2 as the magnetic field is varied is tracked in Figs. 7a through 7c. The appearance of the $\nu=6$ feature at magnetic fields before the $\nu=4$ and 2 features first make their appearance is very surprising, and is a signature of the multi-subband feature of the 3DEG. The assignment of 6 is tentative because from the measured sheet density at zero gate bias and the value of the magnetic field when this minimum is at zero bias, and using the expression $N_s = \nu eB/h$ (where ν is the assigned filling factor, e the electronic charge, and h Planck's constant), one arrives at a filling factor of 6.9. Fig. 7d is a calculation of N_s vs gate voltage deduced from Figs. 7a through 7c.

To understand why such pronounced minima are observed for the narrower PB25 and not for PB24, a self-consistent Poisson-Schrödinger analysis of this system was performed. Potential energies vs depth for four sheet densities (from 0 through $5 \times 10^{11} \text{ cm}^{-2}$) and electron densities vs depth for N_s values of $1 \times, 3 \times,$ and $5 \times 10^{11} \text{ cm}^{-2}$ are shown in Figs. 8a and 8b respectively. At $3 \times 10^{11} \text{ cm}^{-2}$ the second subband is barely occupied and at $5 \times 10^{11} \text{ cm}^{-2}$ the two lowest

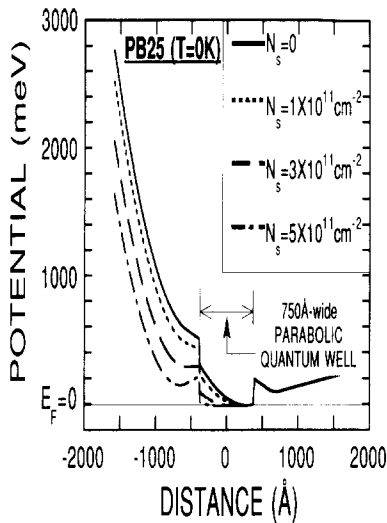


Fig. 8a. Self-consistently calculated potential energies vs depth for 3DEG in 750Å-wide parabolic well (PB25) at different sheet densities (sample surface on left, substrate on right, zero at grown-well-center). Note the square-well shape of the well at the highest density.

subbands are clearly occupied while the third is barely occupied. Note that even in this narrow parabolic well the 3D density is determined by the well curvature once the second subband is occupied. Note also the square-well-like appearance of the self-consistent potential as the electron potential screens out the built-in parabolic potential, especially at the high density of $5 \times 10^{11} \text{ cm}^{-2}$. These features are summarized in Fig. 9 where the subband energies E_i and the sheet density in each subband N_s^i as well as the total density $N_s (= \sum N_s^i)$ are plotted as a function of gate voltage for zero magnetic field. The Fermi energy E_F is the zero energy of the system. Note the pinning of E_F with respect to the bottom of the lowest subband once the second subband is occupied, indicating the 3D nature of this gas. The calculated linear decrease of N_s with negative gate bias is nicely demonstrated experimentally in Fig. 7d. The energy scale pertinent for this sample is of the order of 10meV, allowing minima in the MCV to be observed even at a temperature as high as 4.2K.

The occupation of two subbands with a large intersubband separation should manifest itself in

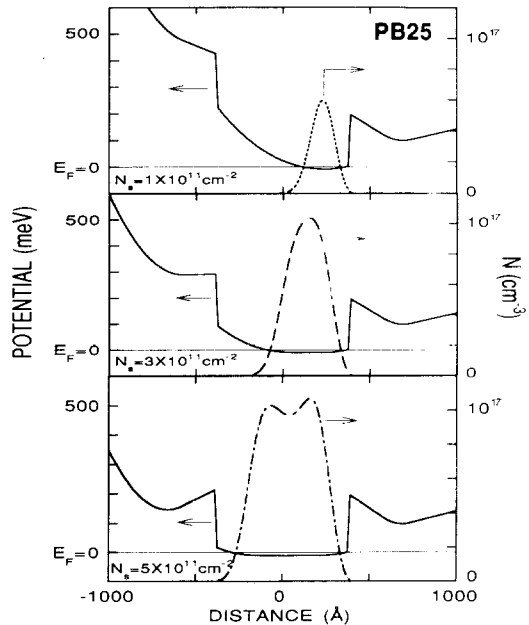


Fig. 8b. Potential energies and total electron density distributions showing three of the cases in Fig. 8a where there is one occupied subband (top), two occupied subbands with the second barely occupied (middle), and three subbands with the third barely occupied (bottom) in the well (PB25).

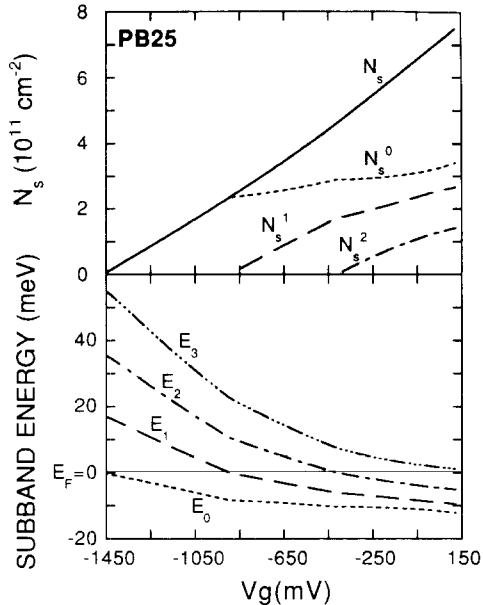


Fig. 9. Subband electron sheet densities and total density (top) and bottoms of subband energies (bottom) as a function of gate bias for PB25. Note the pinning of the Fermi energy with respect to the bottom of the lowest subband once more than one subband is occupied.

transport properties and this is shown in Fig. 10 as a beating of the Shubnikov-de-Haas (SdH) oscillations in the longitudinal resistance of PB25 measured prior to gate deposition (No SdH oscillations were observed for PB24 at 4.2K, where the subbands are separated by less than 1meV). The longitudinal resistance is superimposed on a Landau fan diagram with the zero-field subband energy values self-consistently determined for the measured sheet density ($N_s = 5 \times 10^{11} \text{ cm}^{-2}$ calculated from the minimum of filling factor $\nu = 4$ for which a clear plateau is observed in the Hall resistance). The Fermi energy E_F is the zero of the system and is shown as a constant with magnetic field only as a guide to the eye. As E_F crosses different Landau levels it is clear that some of the minima will be enhanced as opposed to others due to the larger gap between some neighboring Landau levels as opposed to others. Also indicated along the magnetic field axis are the positions of the filling factors ν (deduced from $\nu = 4$) if only one subband were occupied. It is qualitatively clear from this chart that double subband occupancy is responsible for enhancing the minima due to $\nu = 6$ and $\nu = 10$ while suppressing the one due to $\nu = 8$.

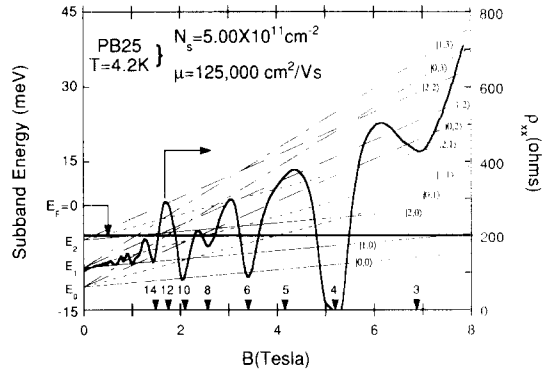


Fig. 10. Landau fan chart constructed for PB25 with zero field values of the bottoms of the subband energies calculated self-consistently for measured sheet density. The Fermi energy (the zero energy of the system) is drawn constant as a guide to the eye. Longitudinal resistance ρ_{xx} is superimposed, and filling factors indicated along the B axis. Non-periodicity in ρ_{xx} shows multiple subband occupancy.

By controlled illumination with an infrared LED it is possible to observe the evolution of the SdH oscillations as N_s is increased from $5 \times 10^{11} \text{ cm}^{-2}$ to $7 \times 10^{11} \text{ cm}^{-2}$. A few of these spectra along with the corresponding Hall resistances are plotted in Fig. 11. The $\nu = 4$ plateau is clearly observed in the Hall resistance in all cases. As N_s increases, the subband energies change, which cause the energy gaps between the Landau levels to change, resulting in turn in changing shapes in the SdH oscillations. For instance, the $\nu = 6$ and $\nu = 8$ minima, and at higher densities the $\nu = 12$ minimum, can be suppressed. From the zero field resistance and the position of the $\nu = 4$ minimum one can calculate electron mobility (parallel to the layers) μ vs N_s . This is shown in Fig. 12. A decrease of μ with increasing N_s is observed and this is qualitatively due to the closer proximity of electrons in the second and third subbands to the ionized impurities in the barriers which are themselves increased in concentration by the illumination. Intersubband scattering effects also perhaps cause this mobility to reduce.

4. CONCLUSION

In conclusion, we have used Capacitance-Voltage measurements in a magnetic field (MCV) to study the electrical properties of a 3-dimensional electron gas (3DEG) system in wide (4640 \AA) and narrow (750 \AA)

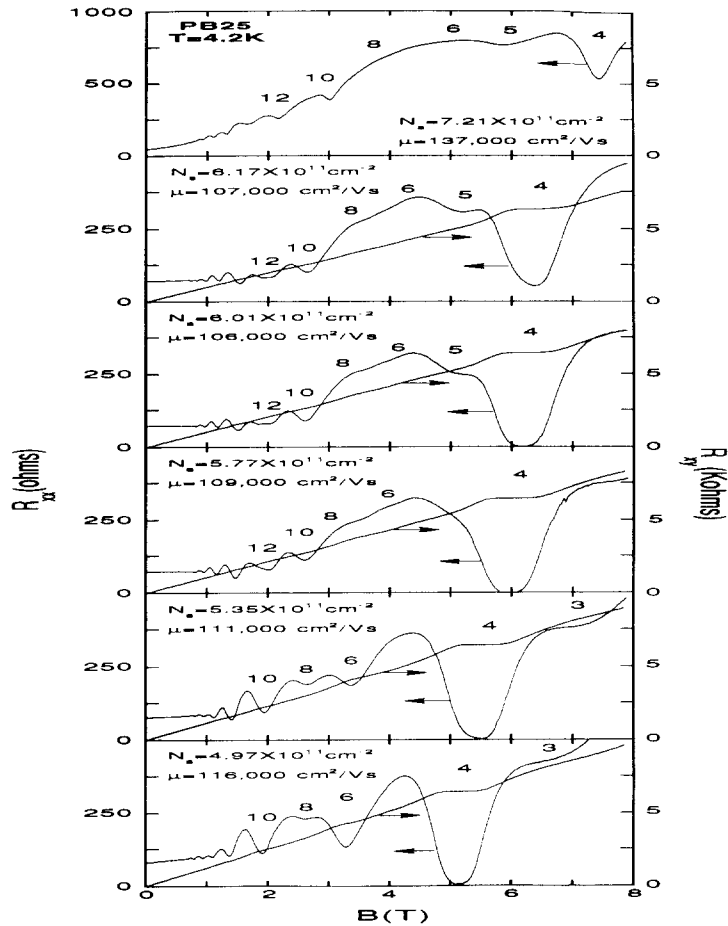


Fig. 11. Evolution of ρ_{xx} and ρ_{xy} (PB25) with increasing illumination (upwards), demonstrating how the ρ_{xx} minima due to filling factors 6 and 8 can be suppressed.

parabolic potential wells. Bumps are observed in the MCV traces at 4.2K for the wide well, their positions in excellent agreement with the biases for subband depopulation but their amplitudes too large by a factor of 5. These bumps persist even when the higher subbands are magnetically depopulated. A calculation of the wavefunctions of the electrons in these 3DEGs in magnetic fields and a deduction of the MCV traces therefrom is obviously necessary. Such calculations have important implications for impurity effects and e^-e^- interactions in the 3DEG.

Minima due to filling factors 2, 4, and 6 (tentative) appear in the MCV traces at perpendicular magnetic fields for electrons in the narrow parabolic well. The

minimum due to 6 appears earlier than the ones due to 2 and 4. The Shubnikov-de-Haas oscillations in the longitudinal resistance reveal non-periodic structure, experimental evidence of multiple-subband occupancy. Mobility (μ) vs sheet density (N_s) measured shows a decrease in μ with increasing N_s over a range of experimental values, suggesting the importance of intersubband scattering mechanisms.

In the narrow parabolic well we have a unique electron gas system: high mobility electrons occupying two subbands with similar densities and with an energy separation that allows structures to manifest themselves in electrical properties even at temperatures as high as 4.2K. It is of great significance

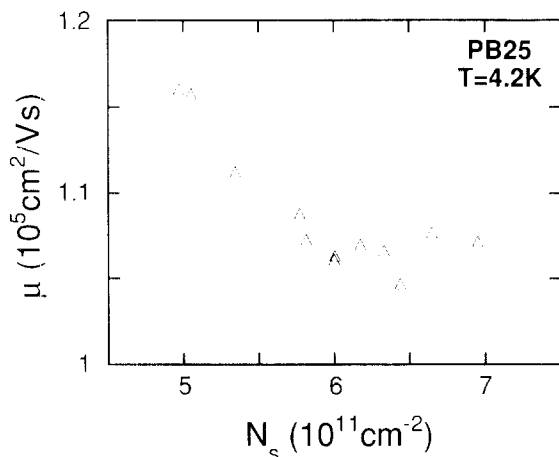


Fig. 12. 4.2K electron mobility vs sheet density for PB25 calculated from the spectra in Fig. 11. Mobility decreases with increasing density, attesting to the influence of electrons occupying the higher subbands in determining the total mobility.

to study the transport properties of these electrons as the dimensionality of the system is tuned from 3D (where the Fermi energy is pinned with respect to the bottom of the lowest subband - a property peculiar to the parabolic well) to 2D (where only the lowest subband is occupied) with a gate. A concurrent measurement of the mobility should afford a sensitive test of intersubband scattering theories. Experiments in these directions are underway and preliminary results are promising.

ACKNOWLEDGEMENTS - We thank R. M. Westervelt, B. Halperin, E. G. Gwinn, P. F. Hopkins, and M. Stopa for valuable discussions. MS also thanks J. H. English for many discussions and valuable hints on MBE growth. This work was supported in part by the U.S. Air-Force Office of Scientific Research under contract # AFOSR-88-0099.

References

1. The original idea was proposed by A. C. Gossard and B. I. Halperin and is reported in B. I. Halperin, Proceedings of the 18th International Conference on Low Temperature Physics, Kyoto, 1987; (Japanese Journal of Applied Physics **26**, Suppl. 26-3, Part 3 (1987)).
2. M. Sundaram, A. C. Gossard, J. H. English, and R. M. Westervelt, Superlattices and Microstructures **4**, 683 (1988).
3. M. Shayegan, T. Sajoto, M. Santos, and C. Silvestre, Applied Physics Letters **53**, 791 (1988).
4. V. Celli and N. David Mermin, Physical Review **140**, Number 3A, A839 (1965).
5. A. H. MacDonald, and G. W. Bryant, Physical Review Letters **58**, 515 (1987).
6. E. G. Gwinn, R. M. Westervelt, P. F. Hopkins, A. J. Rimberg, M. Sundaram, and A. C. Gossard, Physical Review B **39**, 6260 (1989); E. G. Gwinn, P. F. Hopkins, A. J. Rimberg, R. M. Westervelt, M. Sundaram, and A. C. Gossard, Physical Review B **41**, 10700 (1990).
7. T. Sajoto, J. Jo, L. Engel, M. Santos, and M. Shayegan, Physical Review B **39**, 10464 (1989); T. Sajoto, J. Jo, M. Santos, and M. Shayegan, Applied Physics Letters **55**, 1430 (1990).
8. K. Karrai, H. D. Drew, M. W. Lee, and M. Shayegan, Physical Review B **39**, 1426 (1989).
9. L. Brey, and B. I. Halperin, Physical Review B **40**, 11634 (1989).
10. L. Brey, N. F. Johnson, and B. I. Halperin, Physical Review B **40**, 10647 (1989).
11. A. Wixforth, M. Sundaram, K. Ensslin, J. H. English, and A. C. Gossard, Applied Physics Letters **56**, 454 (1990).
12. M. Kawabe, M. Kondo, N. Matsuura, and Kenya Yamamoto, Japanese Journal of Applied Physics **22**, L64 (1983).
13. W. Walukiewicz, M. Sundaram, P. F. Hopkins, A. C. Gossard, and R. M. Westervelt, to be published.
14. G. E. Stillman, private communication.
15. This estimate for n_c was obtained using the Mott criterion, $n_c^{1/3} a_B = 0.25$, where a_B is the Bohr radius: N. F. Mott, Conduction in Non-Crystalline Materials (Oxford University Press, Oxford), 41 (1987).
16. M. Sundaram, A. Wixforth, R. S. Geels, A. C. Gossard, and J. H. English, to be published.
17. T. P. Smith III, B. B. Goldberg, and P. Stiles, Physical Review B **32**, 2696 (1985).
18. V. Mosser, D. Weiss, K. v. Klitzing, K. Ploog, and G. Weimann, Solid State Communication **58**, 5 (1986).